

Modulator noise suppression in the LISA Time-Delay Interferometric combinations

Massimo Tinto,^{*} J. W. Armstrong,[†] and Frank B. Estabrook[‡]

Jet Propulsion Laboratory, California Institute of Technology, Pasadena, CA 91109

(Dated: October 29, 2018)

Abstract

LISA (Laser Interferometer Space Antenna) is a mission to detect and study low-frequency cosmic gravitational radiation through its influence on the phases of six modulated laser beams exchanged between three remote spacecraft. We previously showed how the measurements of some eighteen time series of relative frequency or phase shifts could be combined (1) to cancel the phase noise of the lasers, (2) to cancel the Doppler fluctuations due to non-inertial motions of the six optical benches, and (3) to remove the phase noise of the onboard reference oscillators required to track the photodetector fringes, all the while preserving signals from passing gravitational waves. Here we analyze the effect of the additional noise due to the optical modulators used for removing the phase fluctuations of the onboard reference oscillators. We use the recently measured noise spectrum of an individual modulator (Klipstein *et al.* [1]) to quantify the contribution of modulator noise to the first and second-generation Time-Delay Interferometric (TDI) combinations as a function of the modulation frequency. We show that modulator noise can be made smaller than the expected proof-mass acceleration and optical-path noises if the modulation frequencies are larger than ≈ 682 MHz in the case of the unequal-arm Michelson TDI combination X_1 , ≈ 1.08 GHz for the Sagnac TDI combination α_1 , and ≈ 706 MHz for the symmetrical Sagnac TDI combination ζ_1 . These modulation frequencies are substantially smaller than previously estimated and may lead to less stringent requirements on the LISA's oscillator noise calibration subsystem. The measurements in [1] were performed in a laboratory experiment for a range of modulation frequencies, but we emphasize that, for the reference oscillator noise calibration algorithm to work, the modulation frequencies must be equal to the frequencies of the reference oscillators.

PACS numbers: 04.80.Nn, 95.55.Ym, 07.60.Ly

^{*}Electronic address: Massimo.Tinto@jpl.nasa.gov

†Electronic address: John.W.Armstrong@jpl.nasa.gov

‡Electronic address: Frank.B.Estabrook@jpl.nasa.gov

I. INTRODUCTION

LISA (Laser Interferometer Space Antenna) is a three-spacecraft deep space mission, jointly proposed to the National Aeronautics and Space Administration (NASA) and the European Space Agency (ESA). It will detect and study low-frequency cosmic gravitational radiation by observing frequency shifts of laser beams interchanged between drag-free spacecraft [2].

Modeling each spacecraft with two optical benches, carrying independent lasers, beam splitters and photodetectors, we previously analyzed the measured eighteen time series of frequency shifts (six one-way laser carrier beams between spacecraft pairs, six between the two optical benches on each of the three spacecraft, and six more by over-imposing phase modulations on the laser carrier beams between spacecraft pairs to monitor rates of the reference oscillators on each spacecraft). We showed that there exist several combinations of these eighteen observable which cancel the otherwise overwhelming phase noise of the lasers, and the phase fluctuations due to the non-inertial motions of the six optical benches, and also allow the removal of the phase noise from the onboard reference oscillators (or USOs – "Ultra-Stable Oscillators") required to track the photodetector fringes, while leaving signals due to passing gravitational waves [3].

The analysis in our previous work assumed that noise due to the electro-optic modulators used to implement the onboard reference oscillator noise calibration algorithm was negligible. Here we amend those results to a more realistic LISA operational configuration where the effects of the phase fluctuations of the modulators are explicitly included in the various time-delay interferometric (TDI, [4]) combinations. An experimental investigation for estimating the magnitude of the phase noise introduced by a commercially available electro-optical modulator (EOM) on the phase measurement was recently performed by Klipstein *et al.* [1]. They showed that a modulation frequency of about 8 GHz would be adequate to suppress EOM noise in a one-way phase measurement to smaller than a budgeted noise level. Their conclusion was conservative in that it did not take account of the transfer functions of modulator noise to the TDI combinations. Here we derive the EOM noise transfer functions and show that smaller modulation frequencies than those previously identified could be used, implying less stringent phase noise requirements on the EOMs and perhaps simpler subsystem design.

In Section II we give a brief summary of TDI and its implementation for LISA, and show that the expressions derived in [3] for removing the Ultra-Stable Oscillator noise from the TDI combinations, valid for a stationary LISA configuration (so called “first-generation TDI”), can easily be generalized to the “second-generation” TDI combinations (i.e. those accounting for the the motions of the three spacecraft with respect to each other and around the Sun).

In Section III we derive the transfer functions of the modulator noises to the second-generation TDI combinations X_1 (unequal-arm Michelson), α_1 (Sagnac), and ζ_1 (symmetrized Sagnac). Using the measurements in [1] on a particular EOM, we show that selecting modulation frequencies greater than ≈ 682 MHz (for X_1), ≈ 1.08 GHz (for α_1), and ≈ 706 MHz (for ζ_1) results in the power spectral density of the modulator noise being smaller than the optical-path and proof-mass noises of these TDI combinations.

II. TIME-DELAY INTERFEROMETRY

Equal-arm Michelson interferometer detectors of gravitational waves can observe gravitational radiation by canceling the much larger frequency fluctuations of the laser light injected into their arms. This is done by comparing phases of split beams propagated along the equal (but non-parallel) arms of the detector. The laser frequency fluctuations affecting the two beams experience the same delay within the two equal-length arms and cancel out at the photodetector where relative phases are measured. In this way gravitational wave signals of dimensionless amplitude less than 10^{-22} can be observed using lasers whose frequency stability can be as large as 10^{-13} .

If the arms of the interferometer have different lengths, as will inevitably be the case for space-based detectors such as LISA, simple differencing of the phases on the photodetector does not exactly cancel the laser phase fluctuations, $p(t)$. The larger the difference between the two arms, the larger will be the magnitude of the laser phase fluctuations affecting the detector response. If L_1 and L_2 are the lengths of the two arms, the laser relative phase fluctuations remaining in the response is equal to (units in which the speed of light $c = 1$)

$$\Delta p(t) = p(t - 2L_1) - p(t - 2L_2) . \quad (1)$$

In the case of LISA, whose lasers are expected to display relative frequency fluctuations

equal to about $10^{-13}/\sqrt{\text{Hz}}$ in the milliHertz band, and whose arms will differ by a few percent [2], equation (1) implies the following expression for the amplitude of the Fourier components of the uncanceled laser frequency fluctuations (an over imposed tilde denotes the operation of Fourier transform)

$$|\widetilde{\Delta p}(\omega)| \simeq |\widetilde{p}(\omega)| 2 |\omega| |L_1 - L_2|. \quad (2)$$

At $\omega/2\pi = 10^{-3}$ Hz, for instance, and assuming $|L_1 - L_2| \simeq 0.5$ sec, the uncanceled fluctuations from the laser are equal to $6.3 \times 10^{-16}/\sqrt{\text{Hz}}$. Since the LISA sensitivity goal is about $10^{-20}/\sqrt{\text{Hz}}$ in this part of the frequency band, it is clear that an alternative experimental approach for canceling the laser frequency fluctuations is needed.

The solution of this problem is achieved by first “de-coupling” the two arms with the implementation of a multi-photo-receiver design in which, at each optical bench, the phase difference between the light entering the arm and the one exiting it is measured, time-tagged, and digitally recorded. By then properly time-shifting and linearly combining these phase measurements exact cancellation of the laser phase noise is again achieved. The sensitivity to gravitational radiation for the practical LISA case is essentially equivalent to that of an equal-arm Michelson detector. For a physical and historical description of this technique, called Time-Delay Interferometry (TDI), the reader is referred to [4] and references therein.

In the case of LISA there are six beams exchanged between the three spacecraft, with the six relative phase measurements s_{ij} ($i, j = 1, 2, 3$) recorded when each received beam is mixed with light from an independent laser on the receiving optical bench (that laser also being used to transmit light back along the same arm to the distant spacecraft¹). The frequency fluctuations from all the six lasers, which enter in each of the six Doppler measurements, must be removed to levels smaller than those of the secondary (proof mass and optical path) noises [3] in order to detect and study gravitational radiation at the predicted amplitudes (see Figure 1 for a description of the LISA geometry).

As the three spacecraft forming the LISA array orbit the Sun, their systematic relative motions result in Doppler shifts of the laser frequencies. These offsets may be as large as about ± 20 MHz and are measured at the receiving spacecraft via heterodyning. To limit the

¹ This is the simplest configuration; for technical reasons, schemes in which two or more of the lasers are remotely phase-locked are being considered by the LISA project. TDI works as well for these alternate measurement approaches also [5].

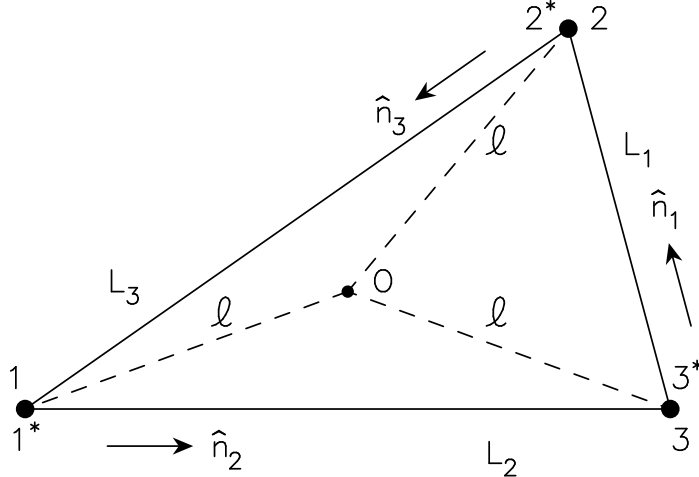


FIG. 1: Schematic LISA configuration. Each spacecraft is equidistant from the point O , in the plane of the spacecraft. Unit vectors \hat{n}_i point between spacecraft pairs with the indicated orientation. At each vertex spacecraft there are two optical benches (denoted $1, 1^*$, etc.), as indicated.

offset frequencies to this range either the lasers must be referenced to an atomic line (such as molecular iodine stabilization [6]) or a sophisticated locking scheme must be employed [5].

A heterodyne measurement is “base-banded” by using a properly selected tracking frequency generated by a reference oscillator (the USO) using servo loop feedback. Although this procedure allows us to accurately track the phases of the photodetector fringes, it introduces into the phase measurements a residual noise due to the USO itself [3]. This USO noise is not negligible and a technique for removing it from the TDI combinations was devised (see [3] for more details). This technique requires the modulation of the laser beams exchanged by the spacecraft, and the further measurement of six more inter-spacecraft relative phases by comparing the sidebands of the received beam against sidebands of the transmitted beam [3].

The time-keeping of the three spacecraft must be synchronized in an inertial frame, usually taken to be the solar system barycentric frame. On each link, the up- and downlink delay times used in the TDI combinations thus differ due to large relativistic aberrations. This is first accommodated in the analysis by so called “modified generation” TDI combinations, and in “second generation” TDI where more general “flexing” of the LISA configuration is allowed. Following [7], the arms are labeled with single numbers given by the opposite space-

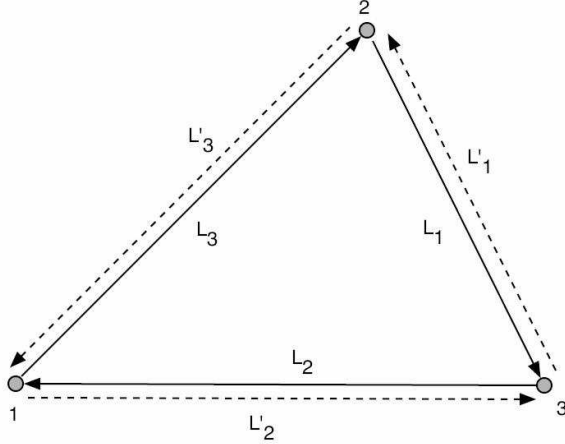


FIG. 2: Schematic diagram of the LISA configuration involving six laser beams. Optical path delays taken in the counter-clockwise sense are denoted with a prime, while unprimed delays are in the clockwise sense.

craft; e.g., arm 2 (or $2'$) is opposite spacecraft 2, where primed delays are used to distinguish light-times taken in the counter-clockwise sense and unprimed delays for the clockwise light times (see Figure (2)). Also the following labeling convention of the relative phase data will be used. Explicitly: s_{23} is the one-way phase shift measured at spacecraft 3, coming from spacecraft 2, along arm 1. Similarly, s_{32} is the phase shift measured on arrival at spacecraft 2 along arm $1'$ of a signal transmitted from spacecraft 3. Due to aberration and the relative motion between spacecraft, $L_1 \neq L'_1$ in general. As in [3], we denote six further data streams τ_{ij} ($i, j = 1, 2, 3$), as the intra-spacecraft metrology data used to monitor the motion of the two optical benches and the relative phase fluctuations of the two lasers on each of the three spacecraft.

The frequency fluctuations introduced by the lasers, by the optical benches, by the proof masses, by the fiber optics, by the USOs, and by the measurements themselves at the photo-detectors (i.e. the shot-noise fluctuations) enter the Doppler observables s_{ij} , τ_{ij} with specific time signatures; see [3, 8] for a detailed discussion. The contribution s_{ij}^{GW} due to GW signals was derived in [9] in the case of a stationary array, and further extended to the realistic configuration [10] of the LISA array orbiting the Sun.

The four data streams recorded at spacecraft 1, including Doppler effects, independent lasers, gravitational wave signals, optical path noises, proof-mass and bench noises, fiber

optics and USO phase fluctuations, are now given by the following expressions [3, 7]

$$s_{31} = \left[\nu_3 (1 - \dot{L}_2) - \nu_1^* - a_{31} f_1 \right] t + p_{3,2} - p_1^* - a_{31} q_1 - \nu_3 \hat{n}_2 \cdot \vec{\Delta}_{3,2} \\ + \nu_3 (1 - \dot{L}_2) \left[2\hat{n}_2 \cdot \vec{\delta}_1^* - \hat{n}_2 \cdot \vec{\Delta}_1^* \right] + s_{31}^{\text{gw}} + s_{31}^{\text{opt. path}} \quad (3)$$

$$\tau_{31} = [\nu_1 - \nu_1^* - c_{31} f_1] t + p_1 - p_1^* - c_{31} q_1 + 2 \nu_1 \hat{n}_3 \cdot (\vec{\delta}_1^* - \vec{\Delta}_1^*) + \mu_1 \quad (4)$$

$$s_{21} = \left[\nu_2^* (1 - \dot{L}_{3'}) - \nu_1 - a_{21} f_1 \right] t + p_{2,3'}^* - p_1 - a_{21} q_1 + \nu_2^* \hat{n}_3 \cdot \vec{\Delta}_{2,3'}^* \\ + \nu_2^* (1 - \dot{L}_{3'}) \left[-2\hat{n}_3 \cdot \vec{\delta}_1^* + \hat{n}_3 \cdot \vec{\Delta}_1^* \right] + s_{21}^{\text{gw}} + s_{21}^{\text{opt. path}} \quad (5)$$

$$\tau_{21} = [\nu_1^* - \nu_1 - c_{21} f_1] t + p_1^* - p_1 - c_{21} q_1 - 2 \nu_1^* \hat{n}_2 \cdot (\vec{\delta}_1^* - \vec{\Delta}_1^*) + \mu_1 . \quad (6)$$

For all the down conversions at spacecraft 1, the USO-generated frequency f_1 is used, and it is multiplied by coefficients a_{21} , a_{31} , c_{21} , and c_{31} that are the result of phase-lock loops driving numerically controlled oscillators to track the large ($\simeq 20$ MHz center frequency) offsets in the heterodyne phase measurements (the ‘‘beat notes’’) [3]. Thus the values of these coefficients are determined by the following expressions

$$a_{31} = \frac{\nu_3 (1 - \dot{L}_2) - \nu_1^*}{f_1} , \quad (7)$$

$$a_{21} = \frac{\nu_2^* (1 - \dot{L}_{3'}) - \nu_1}{f_1} , \quad (8)$$

$$c_{21} = -c_{31} = \frac{\nu_1^* - \nu_1}{f_1} . \quad (9)$$

Eight other relations, for the readouts at vertices 2 and 3, are given by cyclic permutation of the indices in equations (3)-(9).

Recent experimental results have indicated that onboard lasers can be effectively stabilized by referencing their frequency to that of molecular-line transitions such as those defined by molecular iodine (I_2). Besides providing a high reference frequency stability for the LISA onboard lasers, I_2 stabilization has the advantage of making the center frequencies of the lasers onboard each spacecraft essentially equal [6]. In the following we will assume the onboard lasers to be iodine-stabilized, and we will correspondingly set the coefficients c_{ij} defined in equation (9) to be identically equal to zero.

The gravitational wave phase signal components in equations (3) and (5) are given by integrating with respect to time the equations (1), (2) of reference [9], which related frequency

shifts to metric perturbations. It is these that LISA is designed to measure at levels set by the optical path phase noise contributions, $s_{ij}^{\text{opt. path}}$, due mainly to shot noise from the low signal-to-noise ratio (SNR) in the links connecting the distant spacecraft. The τ_{ij} measurements will be made with high SNR so that for them the shot noise is negligible. The other unavoidable secondary phase noise is due to proof mass non-gravitational perturbations, described here by the random displacement vectors $\vec{\Delta}_i$ and $\vec{\Delta}_i^*$.

The expressions of the phase measurements given by equations (3 - 6), when substituted into the second generation laser-noise-free combinations yield data that, although free of laser and motional phase noises, are now affected additionally by the USO phase fluctuations, which have been denoted q_i ($i = 1, 2, 3$) in equations (3 - 6). For instance, with a state-of-the-art USO displaying a frequency stability of about 1.0×10^{-13} in the milliHertz frequency band, the corresponding relative frequency fluctuations, \dot{q}_i/ν_i , introduced in the laser-noise-free data combinations would be equal to about 3.0×10^{-20} , several orders of magnitude above the secondary noises and LISA sensitivity goals [2].

The expressions of the gravitational wave signal, the USO and the secondary noise sources entering into X_1 will in general be different from those entering into X , the corresponding “first generation” unequal-arm Michelson observable derived under the assumption of a stationary LISA array [8, 9]. However, the magnitude of the corrections introduced by the motion of the array on the gravitational wave signal, the USO and the secondary noise sources entering into X_1 will all be proportional to the product of their time derivatives, the spacecraft relative velocities, and the LISA arm-length. At 1 Hz, for instance, the larger corrections (due to aberration) will be about five orders of magnitude smaller than the main terms. Since the amplitude of these corrections scale linearly with the Fourier frequency, we can completely disregard the time- and direction-dependence of the time-delays entering into these noise sources over the entire LISA band [7].

These considerations imply that the second generation TDI expressions for the gravitational wave signal, the USOs and the secondary noises can be expressed in terms of the corresponding first generation TDIs. For instance, the second generation unequal-arm Michelson combination, X_{1q} , (where the q -index indicates the inclusion of the USO noises) can be written in terms of the corresponding first generation unequal-arm Michelson com-

ination, $X_q(t)$, in the following manner [13]

$$X_{1q}(t) = X_q(t) - X_q(t - 2L_2 - 2L_3) , \quad (10)$$

in which the time-dependence of the light-travel times can be completely disregarded. Equation (10) implies that the USO calibration procedure for the second generation TDI combinations can actually be evaluated by simply considering the corresponding calibration expressions derived for the first generation TDI expressions given in [3]. For this reason, from now on we will focus our attention on the first generation combinations.

III. MAGNITUDE OF THE MODULATOR NOISE INTO THE TDI COMBINATIONS

In the USO calibration scheme first proposed by Bender *et al.* [2], a second frequency is superimposed on each of the six main laser beams: specifically, beams originating at spacecraft i are modulated at the frequency f_i generated by its onboard USO. The main carrier signal, together with a side-band (of intensity perhaps ten times lower than the intensity in the carrier [2]) are transmitted, and at the receiving spacecraft j they are heterodyned at a photo detector with the local laser beam ν_j also carrying side-bands [3]. If the frequencies of the sidebands are carefully selected to be larger than the laser frequency offsets (but to differ from each other by an amount smaller than the operational bandwidth of the photo detector) then the lowest two difference frequencies (or difference phase trains) can be distinguished and measured at the photo detector. These two difference phase time series are given respectively by the difference between incoming and outgoing carriers, and by the difference of the phases of their side-bands respectively. They are then independently further tracked with coefficients a_{ij} and b_{ij} [3, 15]. This process provides six additional data records, s'_{ij} . Consider, for instance, the phase difference between the second signal transmitted by bench 3 and the second at the receiving bench 1*

$$\begin{aligned} s'_{31} = & \left[(\nu_3 + f_3) (1 - \dot{L}_2) - \nu_1^* - f_1 - b_{21} f_1 \right] t + p_{3,2} - p_1^* \\ & + q_{3,2} - (1 + b_{21}) q_1 + m_{3,2} - m_1^* \end{aligned} \quad (11)$$

where, for simplicity, we have omitted the terms associated with the optical bench noises, the optical path and proof-mass noises, and the contribution from a possibly present gravitational wave signal. Note that now the expressions for the measurements s'_{ij} include also

the phase noises m_i, m_i^* $i = 1, 2, 3$ introduced by the modulators on the measured phase differences s'_{ij} . These terms were neglected in [3] and here we amend that analysis.

Note that the numerical coefficient b_{21} , determined by the following equation

$$b_{21} = \frac{(\nu_3 + f_3) (1 - \dot{L}_2) - (\nu_1^* + f_1)}{f_1}, \quad (12)$$

is distinct from a_{21} given by equation (7) (although they will be close if all the f_i are close).

The quantities $r_{21}^{(m)} \equiv (s_{21} - s'_{21})/f_3$ and similarly $r_{31}^{(m)} \equiv (s_{31} - s'_{31})/f_2$ (and cyclic permutations of their indices) enter into the algorithm presented in [3] for removing the USO noises from the various TDI combinations. Now they explicitly show their dependence on the modulator noises m_i, m_i^* $i = 1, 2, 3$, and are related to the r_{ij} expressions introduced in [3] (which did not include the modulator noises) by the following expressions

$$\begin{aligned} r_{31}^{(m)} &= r_{31} - \frac{m_{3,2} - m_1^*}{f_3} \\ r_{21}^{(m)} &= r_{21} - \frac{m_{2,3}^* - m_1}{f_2} \end{aligned} \quad (13)$$

with the others obtained as usual via permutation of the spacecraft indices.

A. Modulator Noise in the X -combination

As a result of the presence of modulator noises in the s'_{ij} measurements (and consequently in the combinations $r_{ij}^{(m)}$) the first-generation TDI unequal-arm Michelson combination given in equation (27) of [3] (which now will include combinations of the $r_{ij}^{(m)}$ measurements) will be affected by the modulator noises. If we denote with $X^{(m)}$ the resulting new unequal-arm Michelson combination, it is easy to see that this can be written as the sum of X (as given in [3]) with terms due to the modulator noises. The resulting expression is equal to

$$\begin{aligned} X^{(m)} &= X - a_{12} f_2 \left[\frac{m_{1,22} - m_{2,322}^*}{f_2} + \frac{m_{2,3}^* - m_1}{f_2} + \frac{m_1^* - m_{3,2}}{f_3} + \frac{m_{3,2} - m_{1,22}^*}{f_1} \right] \\ &+ a_{13} f_3 \left[\frac{m_{1,33}^* - m_{3,233}}{f_3} + \frac{m_{3,2} - m_1^*}{f_3} + \frac{m_1 - m_{2,3}^*}{f_2} + \frac{m_{2,3}^* - m_{1,33}}{f_1} \right] \\ &- a_{21} f_1 \left[\frac{m_1^* - m_{3,2}}{f_3} + \frac{m_{3,2} - m_{1,22}^*}{f_1} \right] + a_{31} f_1 \left[\frac{m_1 - m_{2,3}^*}{f_2} + \frac{m_{2,3}^* - m_{1,33}}{f_1} \right] \end{aligned} \quad (14)$$

The expression above leads to the following estimation of the spectral density of the noise, $S_{X^{(m)}}$, in the TDI combination $X^{(m)}$

$$S_{X^{(m)}} = S_X + 4 \sin^2(\omega L) \left[S_{m_1} (a_{12} + a_{13} + a_{31})^2 + S_{m_1^*} (a_{12} + a_{13} + a_{21})^2 + S_{m_2^*} a_{12}^2 + S_{m_3} a_{13}^2 \right] , \quad (15)$$

which has been written as the sum of the secondary noise spectra S_X of the combination X (not containing the modulator noises) and the spectra of the modulator noises themselves. Note that for a figure of merit equation (15) conveniently assumes all USOs to have equal frequency f , and all the armlengths to be equal to a common value L .

Assuming a maximum beat-note frequency offset of 20 MHz in each arm, the coefficients a_{ij} can be taken all equal to $a \equiv 20 \text{ MHz}/f$, where f is the USO or modulation frequency². Given the measured modulator noise spectrum (figure 6 in [1]), from equation (15) it is then possible to determine the value of the USO frequency which would make the modulator noise contribution smaller than the secondary noises ([8], Section IV) affecting the X combination over the entire LISA band. This can be done by maximizing over the angular frequency ω the following function (see equation 15 above)

$$\sin(\omega L) \sqrt{80 \frac{S_m(\omega)}{S_X(\omega)}} \times 20 \text{ MHz} , \quad (16)$$

where $S_m(\omega)$ is the spectrum of the noise associated with one modulator. Over the frequency band relevant to LISA, the measured $S_m(\omega)$ for a single EOM can be approximated by the following analytic expression (see figure 6 in [1])

$$\begin{aligned} S_m(\omega) &= 2.8 \times 10^{-9} \omega^{-1} \text{ cycles}^2 \text{ Hz}^{-1} && \text{when : } 10^{-4} \leq \omega/2\pi \leq 8 \times 10^{-3} \text{ Hz} \\ &= 5.5 \times 10^{-8} \text{ cycles}^2 \text{ Hz}^{-1} && \text{when : } 8 \times 10^{-3} \leq \omega/2\pi \leq 3 \times 10^{-2} \text{ Hz} \\ &= 3.8 \times 10^{-10} \omega^{-3} \text{ cycles}^2 \text{ Hz}^{-1} && \text{when : } 3 \times 10^{-2} \leq \omega/2\pi \leq 5 \times 10^{-1} \text{ Hz} \\ &= 1.2 \times 10^{-11} \text{ cycles}^2 \text{ Hz}^{-1} && \text{when : } 5 \times 10^{-1} \leq \omega/2\pi \leq 1 \text{ Hz} . \end{aligned} \quad (17)$$

Note that the expressions of the power spectral densities of the noises entering into the X , α , and ζ combinations are given in Section IV of [8] as fractional frequency fluctuations,

² In the experimental setup used by [1] to characterize an individual EOM's noise it was not necessary that the modulation frequency be the same as the USO frequency. We emphasize that in LISA's actual USO calibration subsystem the modulation frequency must equal the USO frequency; see Figure 5 of [3].

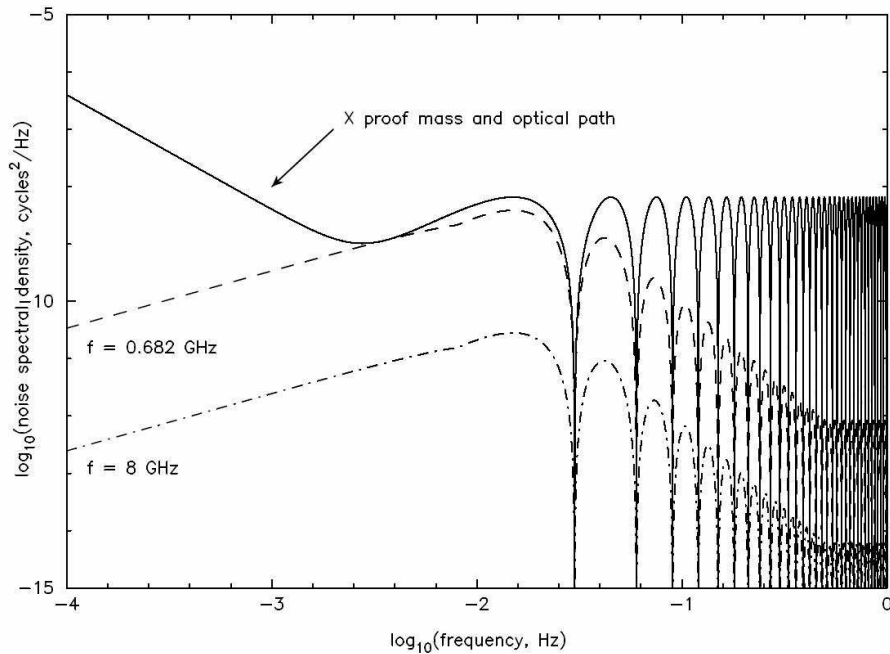


FIG. 3: Numerical comparison of modulation noise in X with a modulation frequency f equal to 682 MHz (dashed-line), 8 GHz (dash-dot line), and the combined secondary noises (solid line).

and therefore need to be converted to the same units as S_m before being used for direct comparison.

After maximizing the function given in equation (16) we conclude that the modulation frequency f should be equal to or larger than 682 MHz for the modulator noise level in the X -combination to be smaller than the remaining secondary noises. A numerical comparison of modulation noise in X at this level, modulation noise if $f = 8$ GHz is adopted, and the combined secondary noises is shown in Fig. 3.

B. Modulator Noise in the α -combination

If we denote with $\alpha^{(m)}$ the resulting new Sagnac combination, it is easy to see that this can be written as the sum of α (as given in [3]) and terms due to the modulator noises. The

resulting expression is equal to

$$\begin{aligned} \alpha^{(m)} = & \alpha + [a_{32} f_2 + a_{13} f_3] \left[\frac{m_1 - m_{2,3}^*}{f_2} \right] - [a_{23} f_3 + a_{12} f_2] \left[\frac{m_1^* - m_{3,2}}{f_3} \right] \\ & - a_{12} f_2 \left[\frac{m_{3,2}^* - m_{2,12}}{f_2} \right] + a_{13} f_3 \left[\frac{m_{2,3} - m_{3,13}^*}{f_3} \right] \end{aligned} \quad (18)$$

The expression above leads to the following estimation of the spectral density of the noise, $S_{\alpha^{(m)}}$, in the TDI combination $\alpha^{(m)}$

$$\begin{aligned} S_{\alpha^{(m)}} = & S_{\alpha} + (a_{32} + a_{13})^2 (S_{m_1} + S_{m_2^*}) + (a_{23} + a_{12})^2 (S_{m_1^*} + S_{m_3}) \\ & + |(a_{13} + a_{12} e^{i\omega L})|^2 S_{m_2} + |(a_{12} + a_{13} e^{i\omega L})|^2 S_{m_3^*} \end{aligned} \quad (19)$$

which has been written as the sum of the noise spectra of the modulator noise-free combination α and the contribution to the overall spectrum coming from the modulator noise. All the armlengths have been taken again to be equal to a common value L .

Again taking the maximum beat-note frequency offset to be 20 MHz in each arm, the coefficients a_{ij} can be treated as all equal to $a \equiv 20 \text{ MHz}/f$. Now the function that needs to be maximized to determine the value of the USO frequency which makes the modulator noise smaller than the LISA secondary noises over the entire LISA band is equal to

$$\sqrt{\frac{S_m(\omega)}{S_{\alpha}(\omega)} (20 + 4 \cos(\omega L))} \times 20 \text{ MHz} . \quad (20)$$

By calculating the maximum value of the above function over the LISA operational band we conclude that a modulation frequency f equal to or larger than $\approx 1.08 \text{ GHz}$ will suppress the modulator noise in the α -combination to a level smaller than the secondary noises. A numerical comparison of the resulting modulation noise in α with the secondary noises is shown in Fig. 4.

C. Modulator Noise in the ζ -combination

We denote with $\zeta^{(m)}$ the new symmetrized Sagnac combination, and write it again as the sum of ζ (as given in [3]) with added terms due to the modulator noises. The resulting

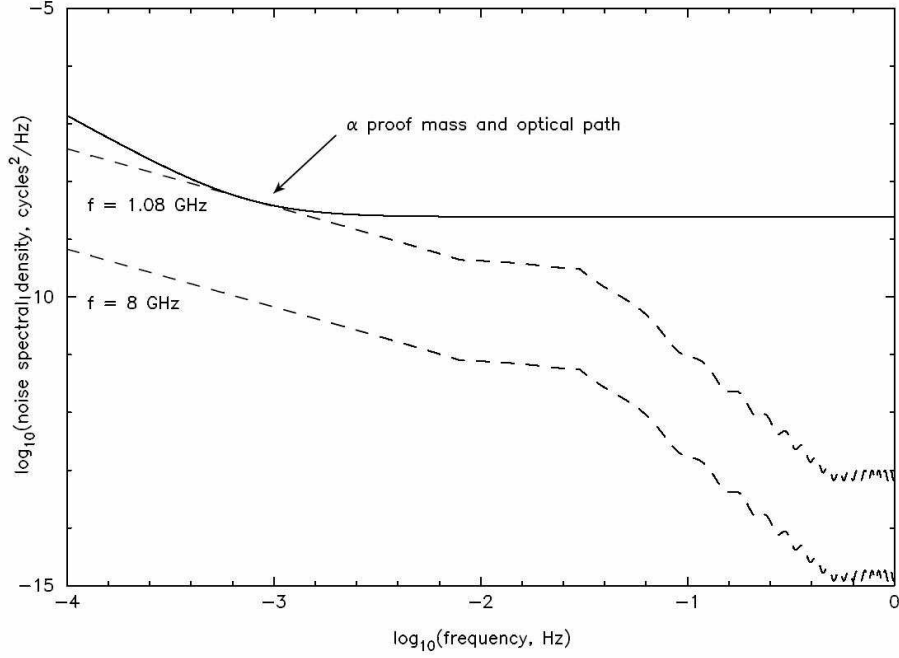


FIG. 4: Numerical comparison of modulation noise in α with a modulation frequency f equal to 1.08 GHz (dashed-line), 8 GHz (dash-dot line), and the combined secondary noises (solid line).

expression is equal to

$$\begin{aligned}
\zeta^{(m)} = & \zeta + \frac{f_1}{3}(a_{21} - a_{31}) \left[\left(\frac{m_{3,3}^* - m_{2,13}}{f_2} \right) - \left(\frac{m_{1,1} - m_{2,31}^*}{f_2} \right) + \left(\frac{m_{2,2} - m_{3,12}^*}{f_3} \right) - \left(\frac{m_{1,1}^* - m_{3,21}}{f_3} \right) \right] \\
& + \frac{f_2}{3}(a_{32} - a_{12}) \left[\left(\frac{m_{1,1}^* - m_{3,21}}{f_3} \right) - \left(\frac{m_{2,2} - m_{3,12}^*}{f_3} \right) + \left(\frac{m_{3,3} - m_{1,23}^*}{f_1} \right) - \left(\frac{m_{2,2}^* - m_{1,32}}{f_1} \right) \right] \\
& + \frac{f_3}{3}(a_{13} - a_{23}) \left[\left(\frac{m_{2,2}^* - m_{1,32}}{f_1} \right) - \left(\frac{m_{3,3} - m_{1,23}^*}{f_1} \right) + \left(\frac{m_{1,1} - m_{2,31}^*}{f_2} \right) - \left(\frac{m_{3,3}^* - m_{2,13}}{f_2} \right) \right] \quad (21)
\end{aligned}$$

In order to identify the minimum modulation frequency f that suppresses the modulator noise below the secondary noises, it is useful to set $a_{ij} = a_{ji}$, which is allowed if there is no flexing and the six lasers are stabilized to the same I_2 transition frequency. Again assuming a maximum beat-note frequency offset of 20 MHz in each arm, the coefficients a_{ij} can be taken as $a \equiv 20 \text{ MHz}/f$. A careful analysis shows that the function which needs to be evaluated to identify the value of the USO frequency f required to make the modulator noise smaller than the LISA secondary noises is

$$\sqrt{\frac{16 [2 - \cos(2\pi fL)] S_m(\omega)}{3 S_\zeta(\omega)}} \times 20 \text{ MHz} . \quad (22)$$

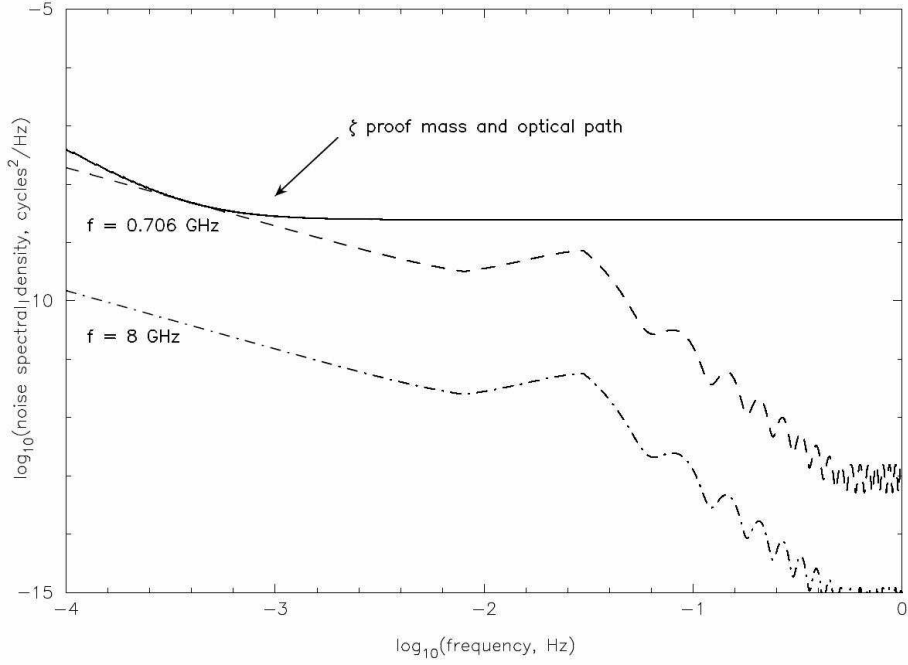


FIG. 5: Numerical comparison of modulation noise in ζ with a modulation frequency f equal to 706 MHz (dashed-line), 8 GHz (dash-dot line), and the combined secondary noises (solid line).

By calculating the maximum value of the function above over the LISA band we conclude that a modulation frequency f equal to or larger than 706 MHz will suppress the modulator noise in ζ to a level smaller than the secondary noises. A numerical comparison of the resulting modulation noise in ζ is shown in Fig. 5.

Acknowledgments

We thank Bill Klipstein, Daniel Shaddock, and Brent Ware for several stimulating discussions about modulator noise. This research was performed at the Jet Propulsion Laboratory, California Institute of Technology, under contract with the National Aeronautics and Space Administration. Massimo Tinto and John Armstrong were supported under research task 05-BEFS05-0014. Frank B. Estabrook is a Distinguished Visiting Scientist at the Jet

- [1] W.Klipstein, P.G. Halverson, R. Spero, R. Cruz, & D. Shaddock. In: *Proceedings of the 6th International LISA symposium*, Editor(s): S.M. Merkowitz and J.C. Livas, AIP Conference Proceedings Volume 873, Greenbelt, Maryland (USA), 19-23 June 2006. ISBN: 978-0-7354-0372-7.
- [2] P. L. Bender, K. Danzmann, and the LISA Study Team, *Laser Interferometer Space Antenna for the Detection of Gravitational Waves, Pre-Phase A Report*, Doc. MPQ 233 (Max-Planck-Institut für Quantenoptik, Garching, 1998).
- [3] M. Tinto, F.B. Estabrook, & J.W. Armstrong *Phys. Rev. D*, **65**, 082003 (2002).
- [4] M. Tinto, and S.V.Dhurandhar, *Living Reviews in Relativity*, **8**, 4 (2005).
- [5] M. Tinto, D.A. Shaddock, J. Sylvestre, & J.W. Armstrong *Phys. Rev. D*, **67**, 122003 (2003).
- [6] V. Leonhardt & J.B. Camp *Appl. Opt.*, **45**, 4142, (2006)
- [7] M. Tinto, F.B. Estabrook, & J.W. Armstrong *Phys. Rev. D*, **69**, 082001 (2004).
- [8] F.B. Estabrook, M. Tinto, & J.W. Armstrong *Phys. Rev. D*, **62**, 042002 (2000).
- [9] J.W. Armstrong, F.B. Estabrook, & M. Tinto *Ap. J.*, **527**, 814 (1999).
- [10] A. Krolak, M. Tinto, & M. Vallisneri *Phys. Rev. D*, **70**, 022003 (2004).
- [11] D.A. Shaddock, M. Tinto, F.B. Estabrook, & J.W. Armstrong *Phys. Rev. D*, **68**, 061303 (2003).
- [12] N.J. Cornish & R.W. Hellings *Class. Quantum Grav.*, **20**, 4851 (2003).
- [13] M. Tinto, & S.L. Larson *Phys. Rev. D*, **70**, 062002 (2004).
- [14] R.W. Hellings, G. Giampieri, L. Maleki, M. Tinto, K. Danzmann, J. Homes, & D. Robertson, *Optics Communications*, **124**, 313, (1996).
- [15] R.W. Hellings, *Phys. Rev. D*, **64**, 022002 (2001).